Fundamental Processes of SF_6 Decomposition and Oxidation in Glow and Corona Discharges

R. J. Van Brunt
and J. T. Herron
National Institute of Standards and Technology,
Gaithersburg, MD

ABSTRACT

It is known that sulfurhexafluoride (SF_6), used as an insulating gas in HV apparatus, will oxidize in electrical discharges in the presence of oxygen or water vapor to form various reactive and stable by-products. In order to meaningfully interpret experimental data on rates of oxidation and by-product formation in discharges, it is necessary to apply theoretical chemical kinetics models that utilize rates for numerous gas-phase processes as functions of gas temperature and/or electric field-to-gas density ratio (E/N). Our current knowledge about the fundamental collision processes involving electrons, ions, free radicals, and molecules needed to understand the gas-phase discharge chemistry in SF_6 is reviewed. Implications of the fundamental rate data reviewed here to recently proposed chemical-kinetics models of corona and glow-type discharges in SF_6 are discussed.

1. INTRODUCTION

OVER the past twenty five years the use of compressed gaseous sulfurhexafluoride (SF_6) as an insulating medium in HV power systems has increased significantly. This gas has a number of favorable properties that make its use acceptable and desirable in such systems. These include its high dielectric strength, chemical inertness, and extremely low toxicity. The fact that SF_6 has, for example, a dielectric strength nearly three times greater than that of air at atmospheric pressure is due to its relatively large cross section for attaching low-energy electrons. Removal of electrons from a gas under electrical stress by formation of negative ions is an important process in inhibiting initiation and growth of electrical discharges.

The high degrees of chemical inertness and thermal stability of SF_6 are due in part to its energetically favorable symmetric, octahedral structure, *i.e.*, the six fluorine atoms are at the corners of a regular octahedron with the sulfur atom at the center. In the gas phase, SF_6 is thermally stable up to about 500°C and will not burn. At temperatures above 150°C it can, however, undergo catalytic decomposition on some types of surfaces. Even when SF_6 is dissociated in an electrical discharge, the products of dissociation tend preferentially to recombine at a rapid rate to reform SF_6. It is this characteristic of SF_6 that also helps to make it a good arc-interrupting medium.

Despite its high level of chemical stability, SF_6 will undergo some degree of decomposition and oxidation in an electrical discharge, particularly when molecular oxygen and water vapor are present. The by-products of SF_6 decomposition are fluorinated gases that can often be quite toxic or corrosive, and there has been increasing concern about the influence that these by-products can have on system reliability and safety. Considerable work has been done in the past fifteen years to identify the products of SF_6 decomposition and measure rates of by-product formation under different conditions. The state of our knowledge about SF_6 decomposition in gas-insulated equipment has been reviewed in several relatively recent publications [1–6] and will therefore, not be covered here.

The purpose of this work is to review progress that has been made in achieving a better understanding of the fundamental gas-phase chemical processes that are responsible for SF_6 oxidation in electrical gas discharges. These are processes that must be considered in any attempt to model the plasma chemistry of discharges or to interpret the results of measurements on the rates of SF_6 decomposition under different conditions. It is known, for example, that the products of SF_6 decomposition in electrical discharges include such species as SF_4, S_2F_{10},

0018-9367/90/0200-75$1.00

SOF_2, SOF_4, SO_2F_2, SO_2, and HF. A theoretical model of the discharge which can account for the observed product distributions and production rates must necessarily include reaction rates for numerous gas-phase collision processes involving electrons, ions, and molecules as functions of temperature and/or electric field-to-gas density ratio E/N.

The focus of the present review is on processes that occur in relatively low-temperature corona, partial discharges or glow-type discharges. Nevertheless, some of the data discussed here may also have relevance to high-temperature discharges such as arcs and sparks [7]. Corona and partial discharges can occur in HV, gas-insulated power equipment; thus decomposition of SF_6 resulting from such discharges is of practical concern [8, 9]. The data on rates of fundamental chemical processes considered in this paper also have application to modeling of glow discharges in SF_6 or SF_6/O_2 gas mixtures used for etching of silicon or other semi-conductor materials [10–15].

The emphasis in this review is on work that has been published during the past ten years.

2. KINETICS MODELS OF GLOW AND CORONA DISCHARGES

In this Section, we shall discuss recent attempts to construct theoretical chemical kinetics models of processes in corona and glow-type discharges for SF_6 and its mixtures with O_2 and H_2O. The emphasis of this discussion is on the high-pressure corona discharge because it is this type that is most relevant to gas-insulated systems. The subsequent sections concerned with rates for fundamental processes are organized in the context of the zonal model for SF_6 corona chemistry considered here.

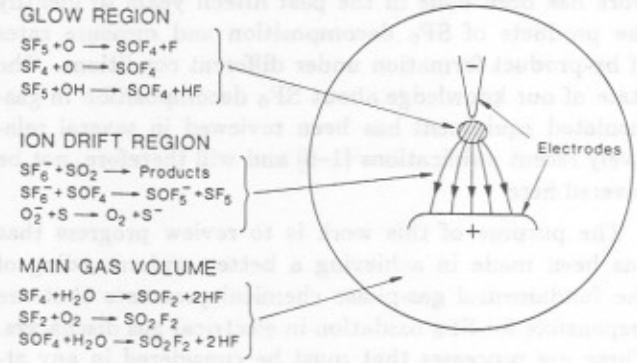

Figure 1.

Regions of differing chemical activity associated with the three-zone model for SF_6 decomposition in negative, point-plane corona.

Recently there have been extensive [3, 16–25] experimental investigations into the decomposition and oxidation of SF_6 in mixtures with various gases like N_2, O_2, Ne, and H_2O using highly localized, point-to-plane, negative glow-type corona discharges. This type of discharge has been described in the literature [26, 27], and is known to have the characteristic that the effective electron temperature (mean electron kinetic energy) in the confined glow region greatly exceeds the gas temperature so that the rate of gas decomposition is controlled primarily by the rates of electron-impact induced molecular dissociation processes such as:

$$e + SF_6 \rightarrow SF_{6-x} + xF + e \qquad x \leq 6 \qquad (1)$$

The glow-type corona has other significant properties, namely: (1) it can be operated with a high level of stability for long periods of time at constant discharge current for a given electrode gap voltage, and (2) it exhibits a well defined region of approximate uniform luminosity near the point electrode. These characteristics make it amenable to theoretical modeling. Chemical decomposition of SF_6 containing trace amounts of oxygen and water vapor in negative glow-type coronas has recently been successfully described using a three-zone chemical-kinetics model of the discharge [28, 29].

Figure 1 shows the three zones of differing chemical activity considered in the negative glow corona model. These zones include: (1) the highly active glow region where E/N is at or slightly above the critical value necessary to sustain ionization thus allowing formation of highly reactive free radials and ions by electron collisions that subsequently react within a relatively short time among themselves or with neutral gas species, (2) the ion-drift region that covers most of the distance between the electrodes, in which charge transport is predominantly by negative ions that may undergo transformations due to ion-molecule reactions, and (3) the main gas volume region surrounding the discharge where slow chemical processes such as gas-phase hydrolysis predominate. It is assumed in this model that the transport of species between zones is controlled by diffusion, which in the case of negative ions, is influenced by the presence of the electric field. A further assumption of the model is that the reaction times of highly reactive free radials such as F and SF_5 are short compared to the times for diffusion out of the glow so that reactions involving these species go to completion in the glow thereby imposing a steady state condition, *i.e.*, the densities of species like F and SF_5 within the glow should be constant in time.

Although the three-zone concept is still considered to be preliminary, it shows promise in accounting for observed yields of oxidation products from corona in SF_6/H_2O and $SF_6/O_2/H_2O$ mixtures as illustrated by results

Table 1.

Reaction Scheme for active corona glow region ($I = 40\ \mu$A) [29].

	Reaction	Rate Coef.
1	$e + SF_6 \rightarrow SF_5 + F + e$	240 1/s
2	$e + SF_6 \rightarrow SF_4 + 2F + e$	1.7 1/s
3	$e + SF_6 \rightarrow SF_2 + 4F + e$	1.4 1/s
4	$e + H_2O \rightarrow H + OH + e$	500 1/s
5	$e + O_2 \rightarrow O + O + e$	14 1/s
*6	$SF_4 \rightarrow SOF_2$	377 1/s
*7	$SF_2 \rightarrow SO_2F_2$	465 1/s
8	$SF_5 + F \rightarrow SF_6$	2.2×10^{-10} cm³/s
9	$SF_5 + SF_5 \rightarrow S_2F_{10}$	6.0×10^{-13} cm³/s
10	$SF_5 + SF_5 \rightarrow SF_4 + SF_6$	5.0×10^{-13} cm³/s
11	$SF_5 + OH \rightarrow SOF_4 + HF$	1.6×10^{-12} cm³/s
12	$SF_5 + OH \rightarrow SOF_4 + F$	2.0×10^{-11} cm³/s
13	$SF_4 + OH \rightarrow SOF_3 + HF$	3.6×10^{-15} cm³/s
14	$SF_2 + O \rightarrow SOF + F$	1.1×10^{-11} cm³/s
15	$SOF + O \rightarrow SO_2F$	1.0×10^{-10} cm³/s
16	$SO_2F + F \rightarrow SO_2F_2$	1.0×10^{-10} cm³/s
17	$SOF + F \rightarrow SOF_2$	2.0×10^{-12} cm³/s
18	$SOF_3 + OH \rightarrow SO_2F_2 + HF$	1.0×10^{-13} cm³/s
19	$F + H_2O \rightarrow OH + HF$	1.1×10^{-11} cm³/s
20	$F + OH \rightarrow FOH$	5.0×10^{-13} cm³/s
21	$H + OH \rightarrow H_2O$	5.0×10^{-13} cm³/s
22	$F + H \rightarrow HF$	1.0×10^{-13} cm³/s
23	$F + F \rightarrow F_2$	2.0×10^{-16} cm³/s
24	$OH + OH \rightarrow H_2O + O$	2.0×10^{-12} cm³/s
25	$H + H \rightarrow H_2$	1.0×10^{-15} cm³/s
26	$F + SOF_3 \rightarrow SOF_4$	1.0×10^{-10} cm³/s
27	$O + SOF_3 \rightarrow SO_2F_2 + F$	5.0×10^{-11} cm³/s

* – diffusion controlled reactions with H_2O or O_2 in main gas volume.

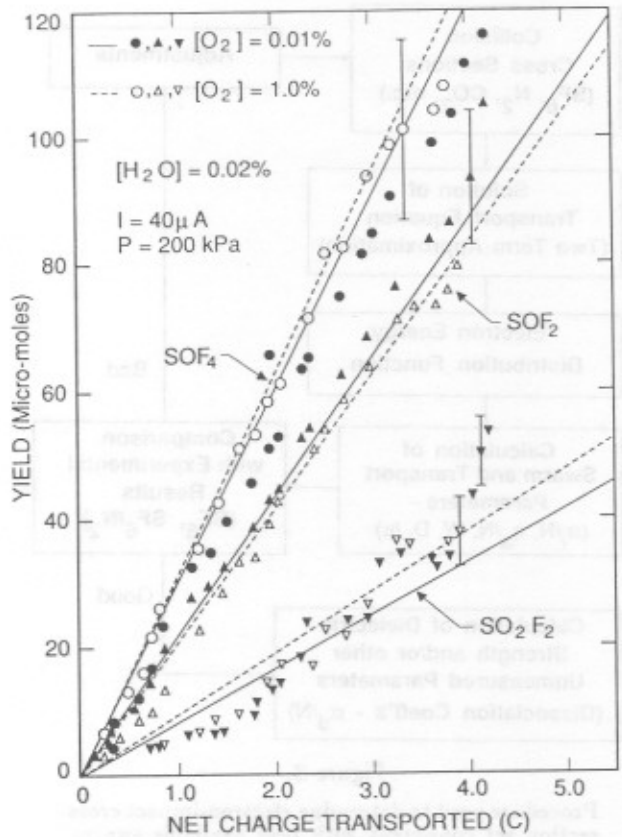

Figure 2.

Calculated (lines) and measured (points) yields of oxyfluorides as a function of net charge transported in the discharge (measured in coulombs) for 40 μA discharge and the indicated oxygen and water vapor concentrations in 200 kPa SF_6.

shown in Figure 2 comparing measured (points) and calculated (lines) yields for the oxyfluorides SOF_4, SOF_2, and SO_2F_2 versus net charge transported (discharge current × time) from a 40 μA negative dc corona in SF_6 containing the various indicated relative amounts of molecular oxygen and water vapor. The set of reactions with corresponding rate coefficients used to obtain the calculated production rates in Figure 2 are listed in Table 1. Admittedly, to achieve the level of agreement with measured data indicated in Figure 2, it was necessary to make some "reasonable" adjustments and guesses of the rate coefficients for several key processes. The rate coefficients given in Table 1 are consistent with expected uncertainties but may not be in complete agreement with our best estimates for these coefficients determined from analysis of fundamental reaction or collision data given later in this work.

It is the general practice when constructing theoretical models of plasma chemistry to begin with the recommended 'best' values for rate coefficients and then adjust these rates within reason to achieve the best agreement with experimental data. The adjustments should generally not significantly exceed the expected or estimated ranges of uncertainties in the rate-coefficient data used. If there are no reasons to seriously question the reliability of the experimental data on chemical processes in a discharge with which the model results are to be compared, then any failure to achieve agreement with experimental data may be due to a failure to include all of the important processes. One must allow for the possibility that there may exist processes of significance that are overlooked simply because there is a lack of knowledge about such processes. In any case, it must be kept in mind that the rate coefficients such as given in Table 1 are, in general, *model specific*. The fact that the rates used in a model give results in satisfactory agreement with the experiment does not prove that the model is unique or complete in the sense that the processes considered are necessarily the only or even the most important processes that can occur in the discharge.

Caution must be exercised in attempting to extract information about rate coefficients for fundamental processes by making adjustments in these coefficients in fit-

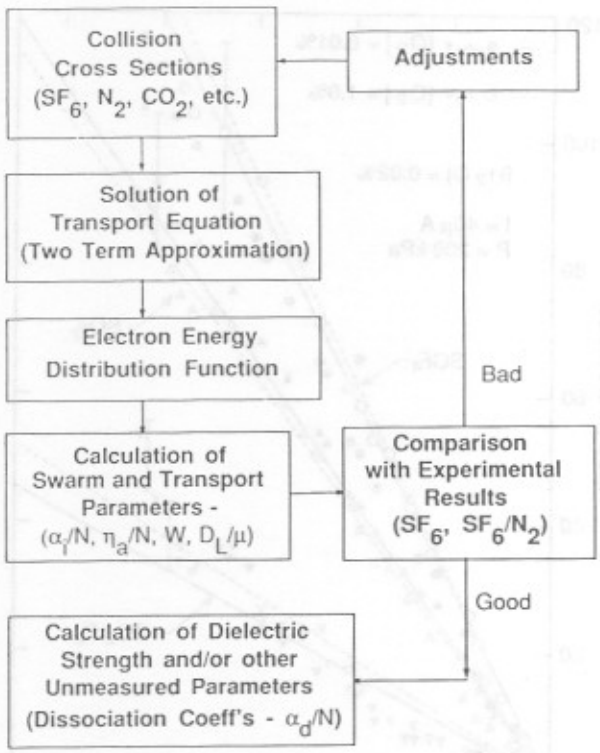

Figure 3.

Procedure used to determine electron-impact cross-section set consistent with best available swarm and transport data from numerical solutions of the Boltzmann transport equation. For definition of symbols used for swarm parameters, [32, 35].

Table 2.

A reaction scheme used in [15] for chemical kinetics model of low-pressure rf discharge in SF_6.

	Reaction	Rate Coef. (cm^3/s)
1	$e + SF_6 \rightarrow SF_6^-$	6.2×10^{-12}
2	$e + SF_6 \rightarrow SF_5^- + F$	2.3×10^{-10}
3	$e + SF_6 \rightarrow F^- + SF_5$	1.5×10^{-10}
4	$e + SF_6 \rightarrow SF_4^- + F_2$	1.5×10^{-11}
5	$e + SF_6 \rightarrow SF_5^+ + F + 2e$	8.5×10^{-9}
6	$e + SF_6 \rightarrow SF_5 + F + e$	3.1×10^{-8}
7	$e + SF_x \rightarrow SF_{x-1} + F + e$	$3.1 \times 10^{-8}(5 \geq x \geq 2)$
*8	$F \rightarrow F(s)$	9.4×10^{-15}
*9	$SF_x \rightarrow SF_x(s)$	3.6×10^{-15}
*10	$SF_x \rightarrow F(s) + SF_{x-1}$	$8.0 \times 10^{-16}(x = 5,3)$
*11	$SF_5^+ \rightarrow SF_5^+(s)$	1.3×10^{-12}
12	$SF_5^+ + SF_5^- \rightarrow 2\,SF_5$	1.0×10^{-7}
13	$SF_5^+ + SF_6^- \rightarrow SF_5 + SF_6$	1.0×10^{-7}
14	$SF_5^+ + F^- \rightarrow SF_6$	1.0×10^{-7}
15	$SF_5^+ + SF_4^- \rightarrow SF_5 + SF_4$	1.0×10^{-7}

* - surface reactions

ting the results of theoretical model calculations to experimental data. For complex plasma-chemical processes involving many reactions, the problem of assessing the

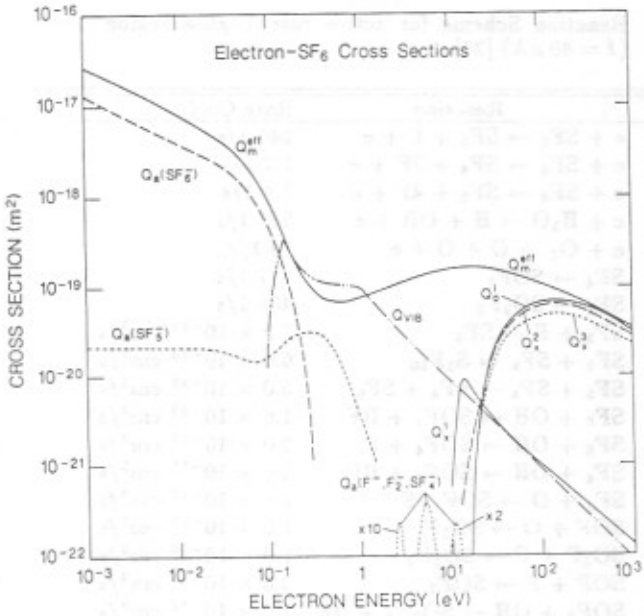

Figure 4.

Electron-SF_6 collision cross sections versus electron energy. Cross section symbols are: Qm^{eff}-effective momentum transfer; $Q_a(SF_6^-)$, $Q_a(SF_5^-)$, and $Q_a(F^-, F_2^-, SF_4^-)$-electron attachment; Q_{VIB}-vibrational excitation; Q_o^i-total ionization; $Q_x{}^j$ $(j = 1,2,3)$-electronic excitation (see Ref. 32).

accuracy and reliability of rates derived in this way may be nearly impossible, or extremely difficult at best. The primary purpose of kinetics models of a discharge should be to test our understanding of the observed phenomena so as to make better assessments of the relative importance of various factors such as gaseous contaminants, surface conditions, and discharge current on the rate of gas decomposition. Theoretical models should be flexible enough that they can be modified or upgraded as more and better fundamental rate data become available.

In addition to the attempt described above to model SF_6 plasma chemistry in high-pressure corona discharges, there have been several attempts to model the chemistry of SF_6 and SF_6/O_2 mixtures in low-pressure diffuse glow discharges such as used for silicon etching [14, 15, 30, 31]. As in the case of corona, this is a low-temperature discharge so that the initial step in the decomposition of SF_6 is electron-impact dissociation (reaction (1)). Because the glow region in such low-pressure discharges encompasses most of the interelectrode gap, a zonal model such as considered for corona is inappropriate. A set of reactions used in the model by Kline [15] for a diffuse rf discharge in pure SF_6 is given in Table 2. It is evident that reactions involving ions and surfaces are assumed to play a more important role in these discharges than in a corona, whereas neutral-neutral recombination processes

are much less important.

In the following sections, we shall examine the state of our knowledge about some of the fundamental collision processes that can occur in the different regions of a glow-type corona discharge. Attention is restricted here to gas-phase reactions, although, as noted above, surface reactions can play an important, and perhaps even a dominant role under some conditions in affecting the observed plasma chemistry. At present, little is known about details of the relevant surface processes that, for example, lead to etching of silicon-containing materials. In gas-insulated systems, the most damaging effect of discharge-induced decomposition of SF_6 is likely to be that associated with the attack on insulating surfaces by reactive species like free fluorine and HF.

3. PROCESSES IN THE GLOW REGION

3.1 ELECTRON-IMPACT DISSOCIATION

As noted in the previous section, electron-impact induced dissociation of SF_6 is the initial rate-controlling step in the decomposition of this gas when subjected to a low-temperature, glow-type discharge. Therefore, in order to make any reasonable estimate of the decomposition rate for SF_6, it is necessary to know the rate coefficient k_d for reaction (1). In general, k_d will depend on E/N and can be calculated if there exists information about the electron-energy dependence of the collision cross sections for dissociative excitation processes and about the E/N dependence of the electron kinetic-energy (ϵ) distribution in the gas. Assuming that there are j different collisional-excitation processes that result in dissociation, k_d is given by [32]

$$k_d\left(\{Q_x^i\}_j\right) = (2/m_e)^{\frac{1}{2}} \sum_{i=1}^{j} \int_{\epsilon_i}^{\infty} Q_x^i(\epsilon) f(\epsilon, E/N) \epsilon \, d\epsilon \quad (2)$$

where m_e is the electron mass, $\{Q_x^i\}_j$, $i = 1, 2, 3, \ldots$, j is the relevant set of dissociative excitation cross sections for SF_6, ϵ_i is the threshold for the ith process, and $f(\epsilon, E/N)$ is the electron kinetic-energy distribution function as computed, for example, from numerical solutions of the Boltzmann transport equation.

Unfortunately, to date there have been no direct measurements or ab-initio calculations of the dissociative-excitation cross sections for SF_6 which can be used to compute k_d. The primary reason that these cross sections have not been measured is because detection of neutral dissociation fragments in their ground state is extremely difficult. Although cross sections for dissociative-excitation processes leading to excited fragments have been measured [33, 34], those processes have high thresholds ($\gtrsim$ 30 eV) and are therefore expected to be relatively unimportant in glow-type discharges where mean electron energies are below about 5 eV.

The lack of data on the $Q_x^i(\epsilon)$ from direct determinations has prompted attempts at indirect determinations using numerical solutions of the Boltzmann transport equation as discussed by Phelps and Van Brunt [32]. In this approach a 'complete' set of electron-collision cross sections is determined which, when used to compute the $f(\epsilon, E/N)$ from the transport equation, gives satisfactory agreement with the best available data on electron swarm and transport parameters such as the ionization and attachment coefficients, drift velocity, and longitudinal and transverse diffusion coefficients (see discussion by L. G. Christophorou and L. A. Pinnaduwage in the present issue [35]). The basic procedure used in this method is illustrated by the block diagram in Figure 3. The initially assumed cross-section set for all electron-impact processes is parameterized in such a way that reasonable adjustments can be made for both shapes and magnitudes of cross sections to achieve best fits to reliable swarm and transport data. In some cases severe constraints must be placed on the range of cross-section adjustments that are made in order to be consistent with reliable information about measured threshold energies, or observed structure in such data as electron-energy loss spectra, optical oscillator strengths, or shapes (energy dependencies) of relative cross sections.

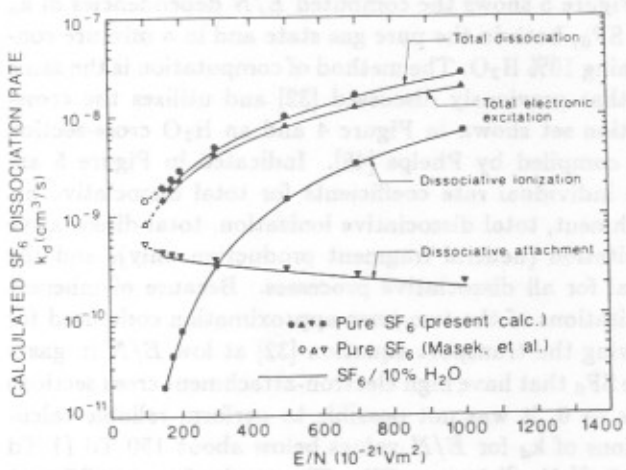

Figure 5.

Calculated electron-impact dissociation rate coefficients for SF_6 in SF_6/10% H_2O (solid lines) and in pure SF_6 (points) as functions of E/N. The following symbols apply for pure SF_6: total dissociation-closed circles, total dissociative ionization-closed squares, total dissociative attachment-closed inverted triangles, calculation of Masek and co-workers at $E/N = 100$ Td-open symbols.

There have been several attempts to determine cross-section sets for SF_6 by this method [36–41]. The SF_6 cross-section set recently proposed by Phelps and Van Brunt [32] is shown in Figure 4 where the notation used is defined in the caption. This cross-section set is optimally consistent with the use of a two-term spherical-harmonic approximation [42] for computing $f(\epsilon, E/N)$ from numerical solutions of the Boltzmann transport equation. Analysis of recent data on electron attachment by Hunter and coworkers [35, 43] suggests that the shape of the SF_6 dissociative-attachment cross section, $Q_a(SF_5^-)$ could be somewhat different from that shown in Figure 4 (see Figure 12b in [35]). However, because this is a relatively weak process, it is not expected to have a significant influence on the computed k_d discussed below. The bases for the Q_x^i shown in Figure 4 are discussed in [32].

In the calculation of k_d using Equation (2) it was assumed, consistent with results [44] for CF_4 and other large fluorinated molecules, that electronic excitation of SF_6 always leads to dissociation, *i.e.*, the cross sections Q_x^i(i = 1, 2, 3) in Figure 4 all correspond to dissociative excitation processes. This assumption is supported by data [33, 45] on ultraviolet and optical emissions from SF_6 excited by electron impact that show either broad, unstructured emission or a predominance of atomic fluorine emission at energies sufficient for electronic excitation. It is known [46, 47] that ionization of SF_6 is always accompanied by dissociation, *i.e.*, SF_5^+ is the largest observed ion fragment even at energies close to the ionization threshold.

Figure 5 shows the computed E/N dependencies of k_d for SF_6, both in the pure gas state and in a mixture containing 10% H_2O. The method of computation is the same as that previously discussed [32] and utilizes the cross-section set shown in Figure 4 and an H_2O cross-section set compiled by Phelps [48]. Indicated in Figure 5 are the individual rate coefficients for total dissociative attachment, total dissociative ionization, total dissociative excitation (neutral fragment production only), and the total for all dissociative processes. Because of inherent limitations of the two-term approximation code used for solving the transport equation [32] at low E/N in gases like SF_6 that have high electron-attachment cross sections as $\epsilon \rightarrow 0$, it was not possible to perform reliable calculations of k_d for E/N values below about 150 Td (1 Td $= 10^{-21}$ Vm^2) in pure SF_6. The results for pure SF_6 are nevertheless seen to be consistent with an extrapolation to k_d values computed by Masek and co-workers [49] at 100 Td. The results in Figure 5 also agree to within a factor of 2 with results of a similar calculation made by Kline [15] using a somewhat different SF_6 cross-section set. Uncertainties of about a factor of 2 are presently considered to be reasonable in such calculations.

The E/N region of greatest importance for glow or

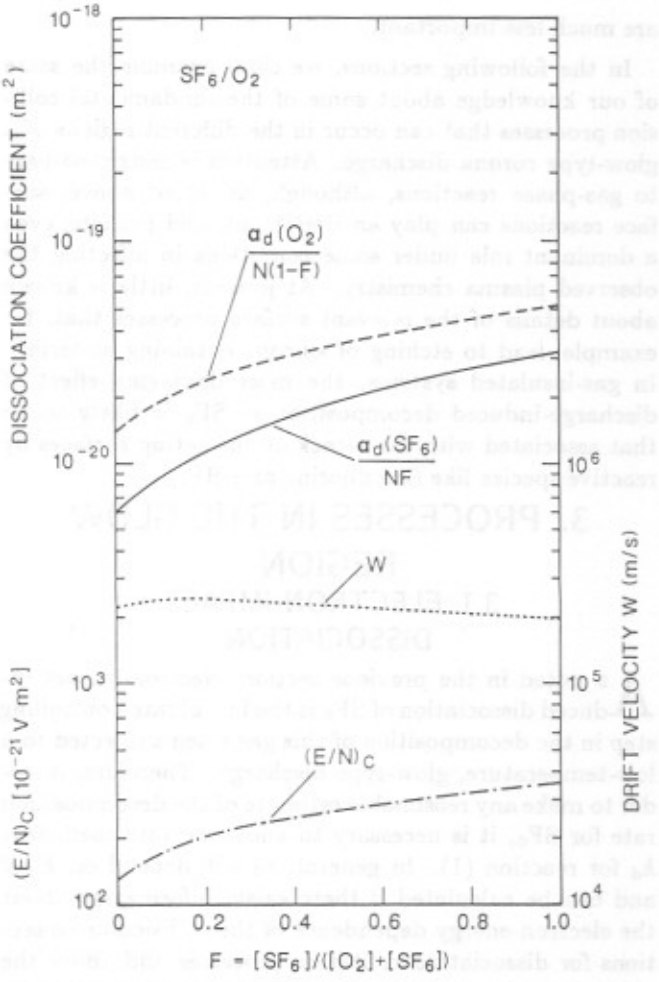

Figure 6.

Calculated dissociation coefficients for SF_6 (solid curve) and O_2 (dashed curve), electron drift velocity (dotted curve) at the critical fields $(E/N)_c$, and $(E/N)_c$ (dot-dashed curve) versus the fractional SF_6 concentration, F, in SF_6/O_2 mixtures (see Ref. 32).

corona discharges is expected to be that close to the critical value, $(E/N)_c = 357$ Td, where the ionization rate in the gas equals the electron attachment rate. In the proposed kinetic models [28, 29] of corona chemistry in SF_6 and mixtures of SF_6 with O_2 and/or H_2O, the active glow region is assumed, consistent with recent observations [50], to be a region where $E/N = (E/N)_c$. The space charge in the steady glow associated with ions and free electrons builds up to a level sufficient to stabilize the discharge and consequently moderate the electric field to the lowest level, $(E/N)_c$, required to sustain ionization. Large deviations of the field from the critical value are expected to result in development of instabilities [51].

As seen in Figure 5, the SF_6 dissociation rate in the region of $(E/N)_c = 357$ Td is dominated by electronic excitation leading to neutral fragments. To obtain results

as shown in Figure 2 from the zonal model of SF_6 decomposition in corona, it was assumed that at $(E/N)_c$ the predominant dissociation channel leads to SF_5 + F fragment formation; however, to properly account for both the SOF_2 and SO_2F_2 yields, it was necessary to assume that approximately 0.7 and 0.6% of the dissociation yields the smaller neutral fragments SF_4 and SF_2 respectively (see Table 1). At the present time there are no direct determinations of the relative degrees of SF_6 dissociation as functions of electron-impact energy or E/N. The only evidence that SF_6 may dissociate directly into relatively small fragments such as SF_2 in a single electron encounter comes from analysis of discharge results as discussed here and in the recent work of Plumb and Ryan [30, 52]. It is evident that acceptable models for SF_6 decomposition in discharges must necessarily consider the relative contributions from all the different energetically available dissociation channels.

Table 3. Enthalpies of Formation at 298 K[a].

Species	$\Delta_f H$, kJ mol^{-1}	Species	$\Delta_f H$, kJ mol^{-1}
F	78.91±1.67	O	249.17±0.10
S	276.98±0.21	SO	5.0±1.3
S_2	128.49±0.29	FO	109±42
SF	13.0±6.3	FO_2	12.6±21
SF_2	−296.6±16.7	F_2O	24.52±1.59
SF_3	−488.3±25	SO_2	−296.84±0.21
SF_4	−763.2±21	OSF	(−207±33)
SF_5	−912.5±13.4	OSF_2	(−494±33)
SF_6	−1220.5±0.8	OSF_3	(−633±21)
S_2F	(−10±20)	OSF_4	(−954±16)
SSF_2	−297±10	OSF_5	(−996±15)
FSSF	−286±10	O_2SF	(−428±15)
$SFSF_3$	−660±24	O_2SF_2	−758.6±8.4
S_2F_6	(−1130±50)	O_2SF_5	−969±15
S_2F_8	(−1570±50)	$(SF_5O)_2$	(−2148±25)
S_2F_9	(−1704±25)	$SF_5O_2SF_5$	(−2069±21)
S_2F_{10}	−2012±21		

a Reference [59]. All values in parentheses are estimated.

It is seen from Figure 5 that the addition of small quantities of water vapor to SF_6 ($[H_2O]/[SF_6] \leq 0.1\%$) has a negligible effect on the calculated dissociation rate coefficients. This is expected since small quantities of any gaseous contaminant in SF_6 should have only a small influence on the electron kinetic-energy distribution at a particular field strength [53–55]. This is also consistent with the observation [56] that low-levels of water contamination in SF_6 have little influence on the uniform-field dielectric strength of the gas. Another quantity related to k_d which is often useful in modeling of discharge processes is the dissociation coefficient, α_d, which essentially represents the number of collisions per electron per unit distance in the gas in the direction of the electric field which result in dissociative excitation of a molecule. It can also be thought of as the inverse of the mean distance in the field direction traversed by an electron between collisions resulting in molecular dissociation. The relationship between α_d and k_d is given by the expression

$$\alpha_d/N = k_d/W \qquad (3)$$

where W is the electron drift velocity in the direction of the field. Like k_d and W, α_d also depends on E/N. Figure 6 shows examples of calculated [32] dissociation coefficients at the critical field $(E/N)_c$ for both SF_6 and O_2 in SF_6/O_2 gas mixtures as functions of mixture ratio $[SF_6]/([O_2] + [SF_6])$. Also shown in this Figure are predicted values of the critical field $(E/N)_c$ and the drift velocity at $(E/N)_c$, both again as functions of mixture ratio. The values given in Figure 6 for dissociation coefficients have been normalized to the corresponding fractional gas component for each species, *i.e.*, divided by $[SF_6]$ for SF_6 and by $[O_2]$ for O_2. The calculations of α_d were made using values of k_d and W obtained from numerical solutions of the Boltzmann transport equation. The SF_6 cross-section set shown in Figure 4 and a slightly modified version of the O_2 cross-section set proposed by Lawton and Phelps [57] were used with the two-term approximation to obtain $f(\epsilon, E/N)$.

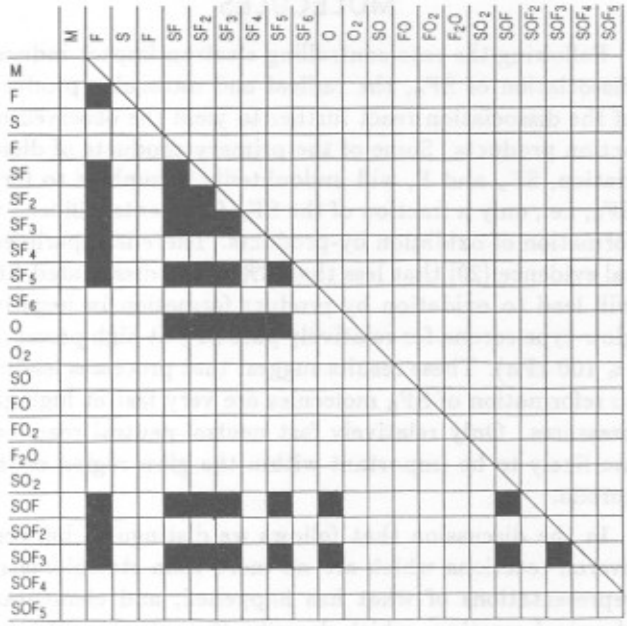

Figure 7.
Reaction grid for the SF_6/O_2 system.

The SF_6/O_2 gas mixture is of particular importance because of its use for plasma etching of silicon and other semiconductor materials in rf glow discharges [10, 14]. We are unaware of any experimental data on either the drift velocity, dissociation coefficients, or $(E/N)_c$ for this mixture. It should be cautioned that in computing $f(\epsilon, E/N)$,

used to obtain the results shown in Figures 5 and 6, it was assumed that changes in the gas composition due to dissociation processes can be neglected. This is equivalent to imposing the requirement of weak decomposition so that the products of decomposition are always at sufficiently low levels that they do not influence the electron kinetic-energy distribution. When applying the results for k_d and α_d shown here to simulations of chemical processes in discharges, one must determine if this assumption of constant gas composition is valid. It may not be valid, for example, in some types of low-pressure microwave discharges in which a significant fraction of the gas in known to be dissociated [58].

It is also important to note that application of α_d or k_d to discharge modeling requires that local equilibrium conditions are satisfied in electron-velocity space so that $f(\epsilon, E/N)$ is properly defined at all times and at all locations in the discharge [35]. Although this may be a problem under special conditions of fast electrical breakdown, in some types of transient discharges, or in regions of highly nonuniform electric fields, it should generally not be a problem in glow-type discharges considered here.

3.2 KINETICS OF UNCHARGED ATOMS, RADICALS AND MOLECULES

Following the rate-controlling electron-impact induced dissociation of SF_6, the radical and molecular products of the dissociation react further to yield the observed reaction products. Some of the primary products of dissociation, SF_x and F, will undoubtedly recombine to form SF_6, *i.e.*, only a fraction of the SF_x fragments will lead to formation of oxidation by-products. There is experimental evidence [20] that less than 3% of the dissociated SF_6 will lead to oxidation by-product formation in negative glow-type corona for relatively pure SF_6 at high pressures ($\leqslant$ 100 kPa). These results suggest that processes leading to reformation of SF_6 molecules are very fast at high gas pressures. Only relatively fast neutral-neutral reactions are likely to be important within the glow region of the corona.

In the discussion that follows we distinguish between overall reactions which are no more than stoichiometric representations of what has happened, and elementary chemical reactions which describe the actual single step processes that take place. The elementary reactions and their associated kinetic parameters are the fully transferable basic data input required to model chemical processes in the glow region of the discharge. In considering these reactions, it is necessary first to devise a strategy to ensure that all important processes are included in the model, and then to compile and evaluate the existing literature data and, in the absence of published experimental or theoretical data, to make reasonable estimates.

$SF_5 + SF_5 \rightarrow SF_6 + SF_4$ (a) $\quad \Delta H(298) = -159$ kJ mol^{-1}
$\rightarrow S_2F_{10}$ (b) $\quad \Delta H(298) = -187$ kJ mol^{-1}

Reference code, notes		Type	T/K	k,k/k(ref) A,A/A(ref)	n	B, B-B(ref)	k err. factor
75TAI/HOW		EX	153-233	1.7E-11		850	
Electron spin resonance. Solvents: $c\text{-}C_3H_8$, CCl_3F_3.							
87HER	(b)	SE		1.7E-11		850	
Recommended	(a)		150-500	1.7E-10		2250	5
	(b)		150-500	1.7E-11		850	3

Comments and Recommendations

There has been only one direct determination of the overall rate of reaction (75TAI/HOW), and no new data have been reported since the last review (87HER). The 87HER recommendation in which the overall reaction at low temperature was attributed entirely to reaction (b) is accepted. However, it should be noted that Schumacher and co-workers (79CZA/SCH, 81GON/SCH) have argued that both (a) and (b) are slow. These arguments are discussed more fully in 87HER.

87HER also proposed a value for the rate constant for reaction (a) which is also adopted here. However, estimates of the combination to disproportionation ratio, k(b)/k(a), are derived from modeling complex systems, such as the pyrolysis of S_2F_{10} (52TRO/MCI, 69BEN/BOT), and are highly unreliable.

References

52TRO/MCI	W. R. Trost and R. L. McIntosh, Can. J. Chem., 29, 508 (1952).
69BEN/BOT	S. W. Benson and J. Bott, Int. J. Chem. Kinetics, 1, 451 (1969).
75TAI/HOW	J. C. Tait and J. A. Howard, Can. J. Chem., 53, 2361 (1975).
79CZA/SCH	J. Czarnowski and H. J. Schumacher, Int. J. Chem. Kinetics, 11, 1089 (1979).
81GON/SCH	A. C. Gonzalez and H. J. Schumacher, Z. Naturforsch., 36 B, 1381 (1981).
87HER	J. T. Herron, Int. J. Chem. Kinet., 19, 129 (1987).

Figure 8.
Example data sheet for the self-reaction of SF_5 radicals.

To identify all possible reactions, we use a reaction grid. This lists along each axis every possible reactant species, which at the intersections defines every possible reaction pair. Furthermore, for every reactant pair we consider every possible set of reaction products. The number of SF_x species to be considered depends on the branching ratios for the primary (and secondary) product yields resulting from the initial electron-impact dissociation event. We allow for all possible kinds of primary products.

Figure 7 shows the reaction grid for the SF_6/O_2 reaction system, which is a subset of the more complete $SF_6/O_2/H_2O$ system. This grid is made up of 22 species which define 242 possible reaction pairs. Many of these reaction pairs can be eliminated by inspection; *e.g.*, $O_2 + O_2$ is obviously not important. Of the remainder, we have made an initial determination of the reactions of greatest importance and indicated them by shaded boxes in Figure 7.

Each reaction pair is treated in terms of a self-contained data sheet. This contains all of the data available for the reaction, and our recommendation for a rate constant to be used in model calculations. Note that all possible products are considered and on the basis of reaction thermochemistry, the probable reaction paths are identified.

The approach is illustrated in Figure 8. The heading of each sheet gives the reactants and the known or postulated products and the reaction enthalpy at 298 K. The reaction enthalpy is calculated from data given in Table 3.

Table 4.

Summary of measured and estimated rate constants for selected atom and radical reactions. These values were either obtained from the indicated references or represent our best estimates (in parentheses). All rate constants apply at 298 K and are in units of cm^3/s. The high-pressure limits are designated with an asterisk.

	Radical or Molecule				
Atom Radical	SF	SF_2	SF_3	SF_4	SF_5
H				4×10^{-10}[75]	2×10^{-10}[75]
O	1.7×10^{-10}[58]	1×10^{-10}[65]	(1×10^{-10})[58]	$< 2\times10^{-14}$[58]	2×10^{-11}[65]
F	(1×10^{-11})	$(5\times10^{-12*})$	(1×10^{-11})	$5\times10^{-12*}$[66]	$9\times10^{-12*}$[66]
OH	(1×10^{-10})	(1×10^{-10})	(1×10^{-10})	(4×10^{-13})	(1×10^{-10})

The data sheet heading is followed by a table giving data from the literature and recommended values. Column 1 contains the reference code and notes relevant to the experimental procedure. The reference code consists of the last two digits of the year of publication, followed by the first three letters of the names of the first and second authors separated by a slash. Column 2 contains a two-character data type code: EX - experimentally measured absolute value; RL - experimentally measured relative value; RN - experimentally measured relative value normalized to an absolute value; TH - theoretical value; DE - derived from modeling study; SE - a recommended value from the literature. Column 3 gives the applicable temperature. If a single temperature is given, *e.g.*, 298 K, the value in Column 4 is k at that temperature; if a temperature range is given, *e.g.*, 200–500 K, the value in Column 4 is the Arrhenius A parameter. The units of k and A are cm^3/s and their values are given in exponential form. Column 5 and Column 6, respectively, contain, when applicable, the n and B parameters in the extended Arrhenius equation, $k = AT^n \exp(-B/T)$. The final entry is the recommended value. Column 7 gives the overall uncertainty factors assigned to k. Following the listing of data there is a section 'Comments and Recommendations', in which the basis for the recommended value is discussed, and the reaction mechanism is treated. Finally, we list the references cited in the data sheet. The complete set of data sheets for all reactions that we have considered will appear elsewhere [60].

As noted above, a serious problem encountered in attempting to set up a truly comprehensive database for modeling plasma chemical processes is the general lack of laboratory data on the reactions of interest. However, that is changing as the interest in explaining and predicting plasma processes on a more fundamental level grows. For example, in the case of the SF_6/O_2 system, Ryan and Plumb (see citations below) are carrying out systematic studies of the mechanisms and kinetics of reactions under low-pressure conditions. Their data are the basis for many of the recommendations given here, and provide the best basis for estimating rate constants for other analogous reactions.

In addition, there are several review articles which provide evaluations of data relevant to plasma chemistry [61–63]. A general source of data is the NIST Chemical Kinetics Database [64]. This is available for use on personal computers using the MS-DOS system (IBM compatible) and includes information on about 2500 reactions contained in over 10000 records. These are mostly reactions of species containing C, H, O, N, and S. Data on reactions of halogens, silicon compounds, and other plasma related species are currently being entered into the system.

Another difficult problem encountered in modeling plasma chemistry is that of estimating rate constants for reactions for which there are no data and for which in many cases there are no reactions that can serve as models. Although it is always preferable to use experimental data as a basis for making a recommendation, failure to provide an estimate is tantamount to setting the rate constant to zero, which is unacceptable. When we make an estimate, we give the basis for it and the kinetic justification. To illustrate the problem, consider the reactions of atoms and radicals with the various SF_x species. Most of these reactions can be described in terms of a general mechanism involving formation of a 'hot' adduct followed by decomposition of the adduct back to reactants, decomposition of the adduct to other products, or formation of a thermalized adduct by collisional stabilization as given by the expressions:

$$A + SF_x \rightleftharpoons [SF_xA]^* \rightarrow B + C$$

$$[SF_xA]^* + M \rightarrow SF_xA + M$$

where M is any gas molecule in the system.

Such data as are available suggest that the radical-radical type reactions are characterized by small or zero activation energies and 'normal' pre-exponential factors. The radical-molecule reactions may be thought of in terms of simple addition reactions, such as the addition of atoms or radicals to multiple bonds of hydrocarbons. These reactions typically have somewhat lower pre-exponential factors and a small but finite activation energy [65].

For purposes of this review, we can treat the reactions in terms of the following categories: (1) atom-radical reactions, (2) radical-radical reactions, (3) radical-self reactions, (4) atom- and radical-molecule reactions.

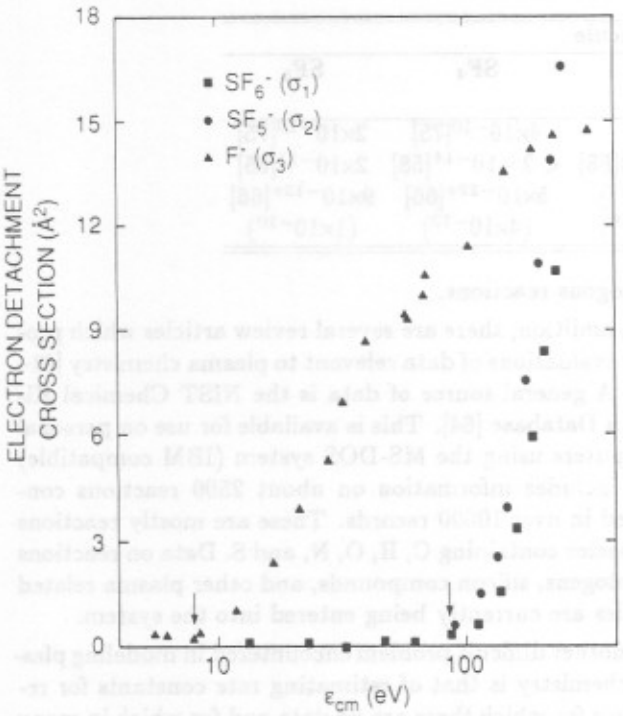

Figure 9.

Measured cross sections for prompt collisional electron detachment for interactions of the negative ions F^-, SF_5^-, and SF_6^- with SF_6 molecules in the ground state [84].

3.2.1 ATOM-RADICAL REACTIONS.

The atom-radical reactions of interest in the SF_6/O_2 system are the reactions of F and O atoms with SF_5, SF_3, and SF. We expect these reactions to be well behaved and thus, by analogy to other reactions of this type, to have rate constants close to the collision rate. This is borne out by the measurements of Plumb and Ryan [66] on the reactions of O atoms with SF_2, SF_5, and SOF. Where there are no direct measurements, we suggest using a rate constant in the range 10^{-10} to 10^{-11} cm^3s^{-1}. Some care must be exercised in using these data, since some of these reactions, *e.g.* $SF_5 + F \rightarrow SF_6$, are reversible association reactions and are pressure dependent [67]. For atmospheric-pressure applications, we assume that the reactions are at or very close to the high-pressure limit. However, since most of the measurements were taken at low pressure and the high-pressure rate constant obtained by fitting the data to some form of theoretically based pressure-dependence equation, the limiting high-pressure value is subject to considerable uncertainty. This problem does not generally exist for reactions such as SF_5+ O $\rightarrow SOF_4 + F$ which, because they are energetically self-contained, need not require third body stabilization and therefore, need not be pressure dependent.

3.2.2 RADICAL-RADICAL REACTIONS.

These are similar to the corresponding atom-radical reactions. Again, on the basis of our knowledge of other radical-radical reactions, we expect the reactions to be very fast, with rate constants in the range 10^{-10} to 10^{-11} cm^3s^{-1} close to the collision limit. Of particular interest are reactions involving OH, for which there are no experimental data. These reactions probably all involve the initial formation of an adduct which then decomposes via a four-center cyclic transition state to yield HF and a sulfuroxyfluoride. This is consistent with what little is known about the properties of the probable adducts. Thus, SF_5OH is known, but the compound is unstable [68]. When formed in a highly exothermic reaction, the adduct has sufficient internal energy to decompose very rapidly. Although no comparable data exist for other OH-containing compounds of this class, we expect them to behave in a similar manner.

3.2.3 RADICAL-SELF REACTIONS.

This is a special class of radical-radical reactions. There is the possibility of combination and of disproportionation, *e.g.*, SF_5+ $SF_5 \rightarrow S_2F_{10}$, the association reaction, and SF_5+ $SF_5 \rightarrow SF_6 + SF_4$, the disproportionation reaction. The SF_5 reaction is the most important in this class since it leads to the formation of the undesirable toxic by-product, S_2F_{10} [6]. Although there are experimental data on some aspects of the SF_5 self-reaction [69–71] and the subject has been reviewed [63], the data are subject to serious interpretive problems, pointing to the need for direct measurements on SF_5 reactions.

For other possible radical-radical reactions, there are few data. If SF and SF_3 are formed in the plasma process, then we should expect to see their association products (and cross products, including cross products with SF_5). The species S_2 [72] and S_2F_2 [73] have been reported as being formed in the plasma dissociation of SF_6. The reactions leading to dimer and cross-product formation should be fast, although it should be noted that the products may also be readily hydrolyzed in the region outside the discharge.

3.2.4 ATOM AND RADICAL-MOLECULE REACTIONS.

These present the greatest problems in terms of estimating rate constants. We are particularly interested in reactions of SF_2 and SF_4 with F, O, and OH. It is known that SF_4 reacts in the condensed phase with a variety of electronegative radicals, X, to generate SF_4X radicals [74]. Unfortunately, that work does not allow us to estimate the relative rate constants for any of these reactions.

There are rate data for the reactions of F atoms with SF_4 [67] and SOF_2 [52] and for the reactions of O atoms with SF_2 [65], SF_4 [58], and SOF_2 [52]. The F atom reactions show some of the same characteristics as the reactions of F atoms with SF_x type radicals. Thus, the reactions of F with SF_4 and SF_2O are pressure dependent, indicating that an adduct is formed which must be collisionally stabilized to be observed. We expect the same kind of behavior for SF_2. The reactions are somewhat slower than radical-radical reactions of F atoms, and we suggest that the reactions will have activation energies in the 5 to 12 kJ mol^{-1} range. For the O atom reactions there is an additional complication in that the ground states of the adducts, *i.e.*, SOF_2 and SOF_4 are singlets, while the reactants must come together on a triplet surface. The products correlate with either the ground singlet state of the adduct or with some excited triplet or singlet (bound?) state. This suggests that ground-state adducts will not be observed. There is no basis for estimating these rate constants. The rate constant for the reaction $O + SF_2$ has been measured by Plumb and Ryan [66] and found to be very fast. However, the same researchers found that the rate constant for the $O + SF_4$ reaction was immeasurably slow [58]. This could mean that the latter reaction has a significant energy barrier or an anomalously low pre-exponential factor.

These observations suggest that although the ground electronic states of SF_2, SF_4, and SF_6 are singlets (*i.e.*, non-free radical in nature), the reactivity varies in the order $SF_2 \gg SF_4 \gg SF_6$. Thus, SF_6 is essentially inert to radical attack; SF_4 reacts slowly with H and even more slowly with O; SF_2 reacts very rapidly with O. We use these observations to predict that SF_2 will be highly reactive with respect to H and OH, whereas SF_4 will be only mildly reactive with respect to OH.

Table 4 summarizes our recommendations for rate constants for use in modeling reactions of atoms and radicals with the SF_x type reactants (not including dimerization reactions). The uncertainties in many of these numbers are large, and for modeling purposes, there is presently considerable latitude in choosing values as inputs to models. As the quantity and quality of the data improve, significant variations in input kinetic data will not be acceptable.

4. PROCESSES IN THE ION-DRIFT REGION

4.1 ELECTRON DETACHMENT AND ION CONVERSION AT HIGH E/N

In the immediate vicinity of the glow region of a corona discharge where E/N is at or close to the critical value $(E/N)_c$, one must consider the possible role of collisional electron-detachment and ion-conversion processes for negative ions associated with SF_6, such as SF_6^-, SF_5^-, and

Table 5.
Ion-molecule reactions at $(E/N)_c = 357$ Td.

Reactions	Rate Coeff's cm^3/s	Reaction Coeff's (cm^2)
Dissociative Ion Conversion:		
$SF_6^- + SF_6 \rightarrow SF_5^- + F + SF_6$	1.25×10^{-12}	1.89×10^{-17} (a)
	1.5×10^{-12}	2.2×10^{-17} (b)
$SF_6^- + SF_6 \rightarrow F^- + SF_5 + SF_6$	4.03×10^{-13}	6.08×10^{-18} (a)
$SF_5^- + SF_6 \rightarrow F^- + SF_4 + SF_6$	2.35×10^{-12}	2.36×10^{-17} (a)
	3.29×10^{-13}	3.3×10^{-18} (b)
	1.4×10^{-12}	1.4×10^{-17} (c)
Charge Transfer:		
$SF_6^- + SF_6 \rightarrow SF_6 + SF_6^-$	1.16×10^{-14}	1.75×10^{-19} (a)
$SF_5^- + SF_6 \rightarrow SF_6^- + SF_5$	2.91×10^{-14}	2.92×10^{-19} (a)
$F^- + SF_6 \rightarrow SF_6^- + F$	1.40×10^{-12}	7.95×10^{-18} (a)
	3.16×10^{-13}	1.8×10^{-18} (b)
	1.2×10^{-12}	6.6×10^{-18} (c)
Prompt Collisional Detachment:		
$F^- + SF_6 \rightarrow F + SF_6 + e$	7.12×10^{-19}	4.05×10^{-24} (a)
$SF_5^- + SF_6 \rightarrow SF_5 + SF_6 + e$	$< 10^{-26}$	$< 10^{-30}$ (a)
$SF_6^- + SF_6 \rightarrow SF_6 + SF_6 + e$	$< 10^{-26}$	$< 10^{-30}$ (a)
Excitation:		
$SF_6^- + SF_6 \rightarrow (SF_6^-)^* + SF_6$	—	—
De-excitation:		
$(SF_6^-)^* + SF_6 \rightarrow SF_6^- + SF_6$	—	—
Auto-detachment:		
$(SF_6^-)^* \rightarrow SF_6 + e$	$\tau^{-1} \geq 10^5/s$	

(a) From Ref. [68]
(b) From Ref. [69]
(c) From Ref. [72]

F^-, in affecting the transport of charge and overall subsequent ion-molecule chemistry in regions of lower E/N. Such reactions may also occur in the relatively high fields of the sheath or cathode fall regions of low-pressure rf or dc glow discharges [77]. The relative magnitudes of the various electron-attachment cross sections for SF_6 shown in Figure 4 indicate that the electrons thermalized in or near the glow by inelastic collisions will most likely attach to SF_6 molecules to form SF_6^- which then becomes the prevalent initial negative-ion charge carrier in the ion-drift region. It should be noted that the SF_6^- formed by low-energy electron collisions with SF_6 is initially energetically unstable and must be stabilized by subsequent collisions with other molecules in the gas. In the case of SF_6, stabilization is very efficient because the unstable negative ion $(SF_6^-)^*$ is known [78–82] to have lifetimes for autodetachment $((SF_6^-)^* \rightarrow SF_6 + e)$ which are usually long compared to mean times between collisions in typical gas-discharge situations. Experimental evidence has also been reported by Foster and Beauchamp [83] that SF_6^- can be stabilized via radiative relaxation $((SF_6^-)^* \rightarrow SF_6^- + h\nu)$.

Some of the negative-ion processes that ought to be considered in the high-field regions of a discharge are

given in Table 5, where the indicated rate coefficients will necessarily have an E/N dependence which can be determined using Equation 2, provided the corresponding cross sections are known. In this case $f(\epsilon, E/N)$ becomes the *ion* kinetic-energy distribution function. Cross sections for collisional-detachment and ion-conversion processes have recently been measured [84] for interactions of F^-, SF_5^-, and SF_6^- with SF_6. These measurements were performed using an ion-beam apparatus and cover the laboratory collision energy range from about 10 to 500 eV. Measured cross sections for 'prompt' collisional electron detachment of the negative ions SF_6^-, SF_5^-, and F^-, which occurs during interaction with SF_6, are shown in Figure 9. The detachment is prompt in the sense that it must occur within 10 μs of the collision. For both SF_6^- and SF_5^-, the prompt collisional-detachment thresholds are unusually high (90 eV), whereas the detachment threshold (8.0 eV) for F^- on SF_6 is comparable to that observed for collisions of F^- with rare gas targets [85]. One reason why SF_6^- and SF_5^- have collisional detachment thresholds significantly above the known electron affinities for these species is due to competition from dissociation processes, *i.e.*, when these ions are excited by collisions, they prefer to dissociate rather than to eject the extra electron.

The measured detachment and ion-conversion cross sections reported in [84] have been used by Olthoff and coworkers [86] to estimate the corresponding reaction rates and coefficients for the same processes. The results of these estimates for $E/N = (E/N)_c$ are given in Table 5 in comparison, where possible, with values extracted from drift-tube measurements [87–90]. In making the estimates reported here for the reaction rates, it was necessary to use a parameterized form for the ion-energy distributions $f(\epsilon, E/N)$ in Equation (2) which were adjusted within reason to achieve consistency with all experimental results. The calculation of reaction coefficients from Equation (3) required use of drift velocities for the ions given by the product of mobility and electric-field strength. There have been many determinations of the mobilities for negative ions in SF_6 [91]. The results in Table 5 were obtained using mobilities for SF_6^- and SF_5^- reported by Brand and Jungblut [92] and the mobility for F^- determined by Nakamura [93].

The rate coefficients for all processes listed in Table 5 exhibit rapid increases with increasing E/N as shown in [86]. An example of the E/N dependence of the reaction coefficient for the collisional dissociation process $SF_6^- + SF_6 \rightarrow SF_5^- + F + SF_6$ is shown in Figure 10. Because of the high threshold energies for the prompt collisional detachment from SF_6^- and SF_5^-, the rates for these processes are found to be negligibly small for $E/N \sim (E/N)_c$, *i.e.*, it can be safely assumed that under normal discharge conditions, prompt collisional detachment from

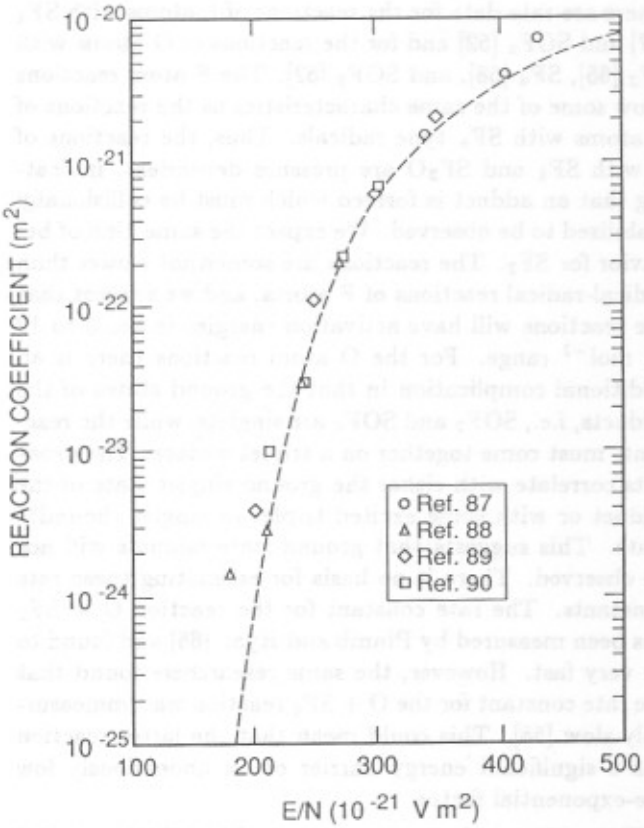

Figure 10.

Comparison of calculated (dashed line) and measured (points) reaction coefficient *vs.* E/N for the collisional dissociation reaction $SF_6^- + SF_6 \rightarrow SF_5^- + F + SF_6$ [86].

either SF_6^- or SF_5^- in their ground states simply does not occur. Previously observed electron detachment during negative-ion drift in SF_6 [87, 94] was most likely due to either F^- or energetically unstable $(SF_6^-)^*$ formed by collisional excitation of SF_6^- or by low-energy electron attachment to SF_6. The rates for collisional excitation and deexcitation of SF_6^- (Table 5) are not known at the present time. The previously observed pressure dependence for the effective electron detachment coefficient of SF_6^- [87, 94] has been recently explained [86] using a kinetics model for negative-ion drift in SF_6 based on the reaction scheme given in Table 3. At low gas pressures the electron detachment occurs mainly from $(SF_6^-)^*$ (autodetachment), whereas at high pressures the detachment occurs mainly from F^- produced by ion-conversion processes. The model predictions are consistent with the high apparent collisional-detachment threshold energies derived by Wiegart [95] from analysis of breakdown probabilities in compressed SF_6. It is the high-pressure situation that is most relevant to the corona discharge phenomena considered here.

Although it has been argued that collisional electron

detachment is, under some conditions, the dominant mechanism for initiation of positive discharges [35, 95, 98], the high thresholds for the detachment of electrons from the fluorinated negative ions that are formed in pure SF_6 suggests that, in contaminated SF_6, collisional detachment occurs mainly from negative ions associated with the contaminants, e.g., negative ions associated with H_2O or O_2. Direct experimental evidence for this has been provided by the measurements of electron avalanche growth [56] and breakdown probabilities [97–99] in SF_6 containing low levels of water vapor and/or oxygen. The formation of negative ions and ion clusters such as $OH^-(H_2O)_n$ $(n = 0, 1, 2)$ have been observed from SF_6 corona discharges as reported in the recent work of Sauers [100]; and it can be expected [56] that collisional electron detachment will occur much more readily from these ions than from F^- or other observed fluorinated negative ions such as $F^-(HF)_n$ $(n = 0, 1, 2, 3, 4)$. The extent to which gaseous contaminants could have influenced results from some previous drift-tube measurements in SF_6 is not entirely clear.

4.2 ION-MOLECULE REACTIONS AT LOW E/N

In contrast to the behavior of the reactions discussed in the previous sections (as illustrated in Figure 10), which exhibit rapid increase of rate with increasing E/N, there exists a class of reactions whose rates decrease with increasing E/N. The maxima in the rates for these types of reactions may actually occur at zero field. It is therefore necessary to consider these reactions in the low-field portion of the ion-drift region of a corona discharge (Figure 1).

An example of a reaction that occurs at low E/N and which can significantly affect the yield of SOF_4 from corona discharges in SF_6 is the 'fast' F^- transfer reaction

$$SF_6^- + SOF_4 \rightarrow SOF_5^- + SF_5 \qquad (4)$$

The E/P (P = pressure) and temperature dependencies of the rate coefficient k for this reaction have been measured [16, 18, 101]. For $T \leq 270$ K, k approaches the collision limit of 2.1×10^{-9} cm^3/s, and for $433 \geq T \geq 270$ K, k decreases with T (K) according to the expression

$$k = 0.124 \exp[-3.3 \ln T] \qquad (5)$$

The E/P dependence of k for a gas temperature of 350 K can be represented by the approximate formula

$$k \sim 7.0 \times 10^{-10} \exp(-0.022 E/P) \qquad (6)$$

where E/P lies within the range 0.5 to 1 V/cm Pa. For $E/P \leqslant 0.5$ V/cm Pa, k assumes an approximate constant value of 2.5×10^{-10}cm^3/s.

Because of the high rate for reaction (4), it is evident [18] that once trace levels of SOF_4 appear in the gas due to discharge-induced oxidation, the most prevalent negative-ion charge carrier in the ion-drift region can change from SF_6^- to $SOF_5{}^-$. It has, in fact, been shown that at low E/N, SF_6^- undergoes rapid F^- transfer not only in reactions with SOF_4 but also with other possible by-products of the discharge such as SiF_4, SO_2, and SF_4. Table 4 shows thermal rate coefficients for various F^- transfer processes at two different gas temperatures that were measured using a pulsed electron-beam in a high-pressure mass spectrometer [16]. The rate constants shown in this Table are consistent with the results from previous rate measurements [101, 102] and with expectations based on F^- affinities of the various molecules [103, 104].

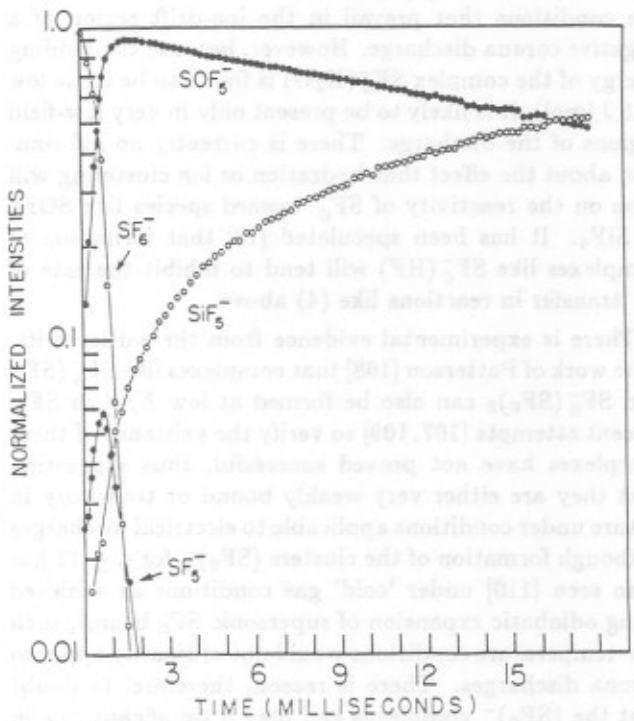

Figure 11.

Normalized ion intensities observed as a function of time following pulsed ionization at 293 K of an SF_6 gas sample previously subjected to a corona discharge and known to contain trace levels of SOF_4 and SiF_4 [16].

The consequences of these reactions on the identity of negative ions in the ion-drift region are illustrated in Figure 11, which shows normalized intensities of negative ions from a high-pressure drift region as a function of time following pulsed ionization by an electron beam in SF_6 containing traces of SOF_4 and SiF_4 produced previously in a corona discharge. The SF_6^- and SF_5^- ions initially produced in the beam rapidly convert to SOF_5^- and SiF_5^- which then become likely terminal ions in the

drift region. It is found [16] in this case that the ratio of ion densities $[SOF_5^-]/[SiF_5^-]$ is ultimately determined at any point by the equilibrium

$$SOF_5^- + SiF_4 \rightleftharpoons SiF_5^- + SOF_4 \quad (7)$$

In addition to the effect of F^- transfer reactions in the ion-drift region, there exists the possibility of negative-ion cluster formation which can also influence ion transport and ion-molecule reaction rates at low E/N. If polar contaminants such as H_2O or HF are present, then it is known [100, 105] that cluster anions such as $F^-(HF)_n$, $SF_6^-(HF)_n$, $SF_6^-(H_2O)_n$, *etc.* are formed. The mean size of the clusters, as given by the integer n, will necessarily tend to decrease as E/N increases [106]. From recent measurements of Sieck [107], it has been shown that the hydrated cluster $SF_6^-(H_2O)$ can be readily formed under the conditions that prevail in the ion-drift region of a negative corona discharge. However, because the binding energy of the complex $SF_6^-(H_2O)$ is found to be quite low (2.5 J/mol), it is likely to be present only in very low-field regions of the discharge. There is currently no information about the effect that hydration or ion clustering will have on the reactivity of SF_6^- toward species like SOF_4 or SiF_4. It has been speculated [18] that formation of complexes like $SF_6^-(HF)$ will tend to inhibit the rate of F^- transfer in reactions like (4) above.

There is experimental evidence from the earlier drift-tube work of Patterson [108] that complexes like $SF_6^-(SF_6)$ and $SF_6^-(SF_6)_2$ can also be formed at low E/N in SF_6. Recent attempts [107, 109] to verify the existence of these complexes have not proved successful, thus suggesting that they are either very weakly bound or transitory in nature under conditions applicable to electrical discharges. Although formation of the clusters $(SF_6)_n^-$ for $n \leq 11$ has been seen [110] under 'cold' gas conditions as achieved using adiabatic expansion of supersonic SF_6 beams, such low-temperature conditions would not ordinarily apply to corona discharges. There is reason, therefore, to doubt that the $(SF_6)_n^-$ complexes can play a significant role in ion transport during corona discharges as previously suggested by Van Brunt and Misakian [111] or that they can have any influence on electron detachment processes at high E/N in SF_6 as proposed by Hansen and coworkers [94].

5. PROCESSES IN THE MAIN GAS VOLUME

THE main gas volume which surrounds the corona discharge (Figure 1) is a region of relatively slow chemistry involving reactive neutral species like SF_4 and SF_2 that diffuse out of the glow. These species can react slowly on the vessel walls or in the gas-phase with likely trace contaminants such as O_2 and H_2O to form oxyfluorides. It has been shown [17] from mass-spectrometric measurements made using the gas mixture $SF_6/O_2/H_2O$ containing either $^{18}O_2$ or $H_2{}^{18}O$ that SOF_2 and SO_2F_2 are formed from negative-glow corona preferentially by reactions respectively with H_2O and O_2. Consistent with these observations, it is suggested [28] that the following slow gas-phase reactions occur in the main gas volume:

$$SF_4 + H_2O \rightarrow SOF_2 + 2HF \qquad k = 1.7 \times 10^{-19} \quad (8)$$

$$SF_2 + O_2 \rightarrow SO_2F_2 \qquad k \leq 5 \times 10^{-16} \quad (9)$$

with k in $cm/^3/s$, and where the rate for reaction (8) has been measured at a temperature of 350 K by Sauers and coworkers [5, 112], and an upper limit for reaction (9) was determined at room temperature by Plumb and Ryan [66]. The experimental evidence [17] is that *most* of the SOF_2 and SO_2F_2 from negative corona discharges in SF_6 and SF_6/O_2 mixtures is produced by reactions (8) and (9) respectively.

Although, the formation of SO_2F_2 seems to require a reaction with molecular oxygen rather than water vapor, it is not clear why SF_2 should react preferentially with O_2 rather than H_2O. More needs to be known about the possible gas-phase reactions involving SF_2. From the early experimental work of Edelson and coworkers [73] there is evidence that SF_2 is a major primary product of high-current arc discharge-induced decomposition of SF_6, whereas S_2F_2 is the major lower sulfur fluoride from low-current discharges. It is also readily produced under some conditions in microwave discharges [113, 114], and although it may be highly reactive or 'unstable' as reported by Seel and coworkers [115], it appears to be energetically stable in the ground state against unimolecular decomposition. Its role in the discharge-induced oxidation of SF_6 is still unclear, and at present reaction (9) must be considered hypothetical.

Table 6.

Rate constants for F^- transfer reactions at 298 K and 373 K

Reactions	Rate Coeff's (cm^3/s) 298 K	373 K
$SF_6^- + SF_4 \rightarrow SF_5^- + SF_5$	7.4×10^{-10}	5.0×10^{-10}
$SF_6^- + SO_2 \rightarrow SO_2F^-, SF_5^-, SO_2F_2^-$	1.06×10^{-9}	8.1×10^{-10}
$SF_6^- + SO_2F_2 \rightarrow$ products	$< 10^{-15}$	$< 10^{-15}$
$SF_6^- + SOF_2 \rightarrow$ products	$< 10^{-15}$	$< 10^{-15}$
$SO_2F^- + SOF_4 \rightarrow SOF_5^- + SO_2$	6.8×10^{-10}	3.9×10^{-10}
$SF_6^- + SOF_4 \rightarrow SOF_5^- + SO_2$	8.5×10^{-10}	4.0×10^{-10}
$SF_6^- + SiF_4 \rightarrow SiF_5^- + SF_5$	5.6×10^{-10}	5.6×10^{-10}

The oxyfluorides SOF_2 and SOF_4 can also hydrolyze via the slow gas-phase reactions (with k in cm^3/s)

$$SOF_2 + H_2O \rightarrow SO_2 + 2HF \qquad k = 1.2 \times 10^{-23} \quad (10)$$

$$SOF_4 + H_2O \rightarrow SO_2F_2 + 2HF \qquad k = 2.0 \times 10^{-21} \quad (11)$$

The rate coefficients for these reactions were measured at a gas temperature of 298 K by Van Brunt and Sauers

[116]. Although these processes could have long-term effects on observed relative concentrations of the oxyfluorides produced during electrical discharges in SF_6, the rates are obviously quite low, and there are indications from measurements [3, 17, 117] of gaseous by-product concentrations during operation of discharges that reactions (10) and (11) in the gas phase cannot account for the observed production of the species SO_2 and SO_2F_2. There is evidence [3, 112, 118] that hydrolysis of SF_4, SOF_2, and SOF_4 can occur relatively more rapidly in liquid H_2O or on surfaces containing adsorbed H_2O. A large discrepancy exists between the SOF_2 hydrolysis rate reported by Van Brunt and Sauers [116] and the rate reported by Ruegsegger and coworkers [4]. This undoubtedly arises because, in the latter case, which was an indirect measurement involving short-time mass spectrometric observations of a 'complete' SF_4 hydrolysis, the possibility existed for surface reactions with H_2O that need not involve SOF_2 as an intermediate [116]. It has been suggested [3] that hydrolysis of SOF_4 could occur sufficiently rapidly on surfaces so as to preclude its observation in some experiments [22, 24, 25].

In relatively pure SF_6, the direct production rate of SO_2 from corona discharges is found to be quite small [3]. It can, however, become a major by-product in binary mixtures like SF_6/N_2 or SF_6/Ne in which SF_6 is the minor component [20]. When significant quantities of H_2O are present on surfaces, the SO_2 produced in the discharge or by hydrolysis of SOF_2 can itself be hydrolyzed by the reaction

$$SO_2 + H_2O \rightarrow H_2SO_3 \qquad (12)$$

In general, it can be expected that for species like SF_4, SOF_2, SOF_4, and SO_2, surface reactions will begin to predominate over gas-phase reactions as the surface-to-volume ratio is increased for any enclosed SF_6-insulated systems.

There is recent conclusive experimental evidence [21, 119] that the production and detection of gaseous S_2F_{10} from electrical discharges in SF_6 can also be affected by surface reactions. There is particular concern about the production of this species because of its known high level of toxicity [6]. It is formed by reaction of SF_5 free radicals at high gas pressure (Table 1) whenever SF_6 is dissociated. Although it is thermally stable at 300 K, it will react at this temperature with H_2O adsorbed on surfaces to form a variety of products which may include SOF_2, SO_2, HF, and SF_6, depending on surface conditions. Little is known at present about the exact nature of S_2F_{10} decomposition which occurs via surface catalyzed reactions. It is nevertheless important to understand more about these processes because they could significantly effect one's ability to reliably perform a quantitative analysis of SF_6 to determine the presence of S_2F_{10} [119].

6. CONCLUSION

THE basic reactions among electrons, ions, and molecules that lead to formation of permanent, stable or long-lived by-products of SF_6 decomposition and oxidation in low-temperature glow-type discharges have been reviewed in the context of a zonal model for highly localized negative coronas. In the active glow region of the discharge, the initial rate-controlling reaction is dissociation of SF_6 by electron impact, the rate for which has been estimated using numerical solutions of the Boltzmann Transport Equation. It is this reaction which sets an upper limit on the total rate of SF_6 decomposition under any given set of discharge conditions [3]. The initial dissociation is followed by relatively fast reactions involving the products of dissociation, namely free fluorine and the lower-valence sulfur fluorides. Reactions leading to reformation of SF_6 appear to predominate in relatively pure SF_6. Reactions of the SF_6 dissociation products among themselves and with O_2 or H_2O can lead to formation of a variety of long-lived corrosive or toxic by-products, especially S_2F_{10}, SOF_4, and HF. Some of the relatively stable lower-valence sulfur fluorides such as SF_2 and SF_4 may escape the glow region and eventually react slowly with contaminants like H_2O or O_2 in the main gas volume to form by-products such as SO_2F_2 and SOF_2. Negative ions formed in the discharge can also react preferentially with the products of oxidation and thereby significantly affect the yields of these products.

Presently our knowledge about the rates for several key reactions must be considered meager or highly uncertain at best. Although considerable progress has been made, especially during the past ten years, in identifying important reactions and in measuring or computing their rates, it is still necessary, in the construction of theoretical plasma-chemical models of glow discharges, to make guesses about rates for numerous processes that are deemed to be important or probable from simple energetic considerations or from analogies with known reactions in systems that are judged to be chemically or structurally similar. From attempts to model the chemistry in glow-type discharges, it becomes evident that more information is needed on branching ratios for different SF_6 dissociation channels leading to formation of different fragments, SF_x, $x \leqslant 5$. Little is presently known about reactions of SF_x species with free radicals like OH, even though such reactions are expected to be quite important in the glow region. More data is needed on the chemistry of SF_2 in the presence of O_2 since it is believed to be an important precursor to formation of SO_2F_2. Surface catalyzed hydrolysis reactions of S_2F_{10}, SOF_4,

[46] J. K. Olthoff, R. J. Van Brunt and I. Sauers, "Electron-Energy Dependence of the S_2F_{10} Mass Spectrum", J. Phys. D: Appl. Phys., Vol. 22, pp. 1399–1401, 1989.

[47] B. P. Pullen and J. A. D. Stockdale, "Dissociative Ionization of SF_6 by Electron Impact", Int. J. Mass Spec. and Ion Physics, Vol. 19, pp. 35–42, 1976.

[48] A. V. Phelps (private communication).

[49] K. Masek, L. Laska, V. Perina and J. Krasa, "Some Peculiarities of the SF_6 and the $SF_6 + O_2$ Discharge Plasma", Acta Phys. Slov., Vol. 33, No. 3, pp. 145–150, 1983.

[50] D. B. Ogle and G. A. Woolsey, "Diffuse and Constricted Glow Discharges in SF_6", J. Phys. D: Appl. Phys., Vol. 20, pp. 453–461, 1987.

[51] L. Niemeyer, "A Model of SF_6 Leader Channel Development", Proc. 8th Int. Conf. on Gas Discharges and Their Application, Leeds University Press, UK, pp. 223–226, 1985.

[52] I. C. Plumb and K. R. Ryan, "Gas-Phase Reactions in Plasmas of SF_6 with O_2: Reactions of O with SOF_2", Plasma Chem. Plasma Proc., Vol. 9, No. 3, pp. 409–420, 1989; K. R. Ryan, "Aspects of the Chemistry of SF_6/O_2 Plasmas", Plasma Chem. Plasma Proc., Vol. 9, No. 4, pp. 483–496, 1989.

[53] M. F. Fréchette and J. P. Novak, "Boltzmann-Equation Analysis of Electron Transport Properties in $CCl_2F_2/SF_6/N_2$ Gas Mixtures", J. Phys. D: Appl. Phys., Vol. 20, pp. 438–443, 1987.

[54] M. F. Fréchette and J. P. Novak, "Limit Field Behavior of Various Gas Mixtures Discussed in the Framework of Boltzmann-Equation Analysis", IEEE Trans. Elec. Insul., Vol. 22, pp. 691–698, 1987.

[55] R. J. Van Brunt, "Common Parameterizations of Electron Transport, Collision Cross Section, and Dielectric Strength Data for Binary Gas Mixtures", J. Appl. Phys., Vol. 61, No. 5, pp. 1773–1787, 1987.

[56] R. J. Van Brunt, "Water Vapor-Enhanced Electron-Avalanche Growth in SF_6 for Nonuniform Fields", J. Appl. Phys., Vol. 59, No. 1, pp. 2314–2323, 1986.

[57] S. A. Lawton and A. V. Phelps, "Excitation of the $b^1\Sigma_g^+$ State of O_2 by Low-Energy Electrons", J. Chem. Phys., Vol. 69, No. 3, pp. 1055–1068, 1978.

[58] K. R. Ryan and I. C. Plumb, "Gas-Phase Reactions in Plasmas of SF_6 with O_2 in He", Plasma Chem. Plasma Proc., Vol. 8, No. 3, pp. 263–280, 1988.

[59] J. T. Herron, "Thermochemical Data on Gas Phase Compounds of Sulfur, Fluorine, Oxygen and Hydrogen Related to Pyrolysis and Oxidation of Sulfurhexafluoride", J. Phys. Chem. Ref. Data, Vol. 16, No. 1, pp. 1–6, 1987.

[60] J. T. Herron, in preparation.

[61] W. Tsang and R. F. Hampson, "Chemical Kinetic Data Base for Combustion Chemistry. Part 1. Methane and Related Compounds", J. Phys. Chem. Ref. Data, Vol. 15, No. 3, pp. 1087–1279, 1987.

[62] R. Atkinson, D. L. Baulch, R. A. Cox, R. F. Hampson, Jr., J. A. Kerr and J. Troe, "Evaluated Kinetic and Photochemical Data for Atmospheric Chemistry: Supplement III", IUPAC Sub-committee on Gas Kinetic Data Evaluation for Atmospheric Chemistry, J. Phys. Chem. Ref. Data., Vol. 18, No. 2, pp. 881–1097, 1989.

[63] J. T. Herron, "A Critical Review of the Chemical Kinetics of SF_4, SF_5, and S_2F_{10} in the Gas Phase", Int. J. Chem. Kinet., Vol. 19, No. 2, pp. 129–142, 1987.

[64] NIST Standard Reference Database 17, "NIST Chemical Kinetics Database", Office of Standard Reference Data, National Institute of Standards and Technology, Gaithersburg, MD, 1989.

[65] S. W. Benson, *Thermochemical Kinetics*, Wiley, NY, 1976.

[66] I. C. Plumb and K. R. Ryan, "Gas-Phase Reactions of SF_2, SF_4, and SOF with $O(^3P)$: Their Significance in Plasma Processing", Plasma Chem. Plasma Proc., Vol. 6, No. 3, pp. 247–258, 1986.

[67] K. R. Ryan and I. C. Plumb, "Gas-Phase Combination Reactions of SF_4 and SF_5 with F in Plasmas of SF_6", Plasma Chem. Plasma Proc., Vol. 8, No. 3, pp. 281–292, 1988.

[68] K. Seppelt, "Pentafluoro-orthosulfuric Acid, $HOSF_5$, and its Higher Homologues", Z. anorg. allg. Chem., Vol. 428, pp. 35–42, 1977.

[69] W. R. Trost and R. L. McIntosh, "The Kinetics of the Thermal Decomposition of Disulfur Decafluoride", Can. J. Chem., Vol. 29, pp. 508–525, 1951.

[70] S. W. Benson and J. Bott, "The Kinetics and Thermochemistry of S_2F_{10} Pyrolysis", Int. J. Chem. Kinet., Vol. 1, No. 5, pp. 451–458, 1969.

[71] J. C. Tait and J. A. Howard, "An Electron Spin Resonance Study of Some Reactions of Pentafluorosulfuranyl (SF_5)", Can. J. Chem., Vol. 53, No. 16, pp. 2361–2364, 1975.

[72] K. E. Greenberg and P. J. Hargis, Jr., "Detection of Sulfur Dimers in SF_6 and SF_6/O_2 Plasma-Etching Discharges", Appl. Phys. Lett., Vol. 54, No. 14, pp. 1374–1376, 1989.

[73] D. Edelson, C. A. Bieling and G. T. Kohman, "Electrical Decomposition of Sulfurhexafluoride", Ind. Eng. Chem., Vol. 45, No. 9, pp. 2094–2096, 1953.

[74] J. R. Morton and K. F. Preston, "An EPR Study of the Addition of Oxy-Radicals to Sulphur Tetrafluoride", Chem. Phys. Lett., Vol. 18, No. 1, pp. 98–101, 1973.

[75] R. J. Malins and D. W. Setser, "Rate Constants and Vibrational Energy Disposal for Reaction of H Atoms with Br_2, SF_5Br, PBr_3, SF_5 and SF_4", J. Chem. Phys., Vol. 73, No. 11, pp. 5666–5680, 1980.

[76] J. Brunning and M. A. A. Clyne, "Elementary Reactions of the SF Radical. Part 1. Rate Constants for the Reactions F + OCS → SF + CO and SF + SF → SF_2 + S", J. Chem. Soc., Faraday Trans. 2, Vol. 80, pp. 1001–1014, 1984.

[77] B. Chapman, *Glow Discharge Processes*, John Wiley and Sons, New York, 1980.

[78] S. P. Heneghan and S. W. Benson, "Kinetics and Thermochemistry of Electron Attachment to SF_6", Int. J. of Chemical Kinetics, Vol. 15, pp. 109–117, 1983.

[79] P. W. Harland and J. C. J. Thynne, "Autodetachment Lifetimes, Attachment Cross Sections, and Negative Ions Formed by Sulfurhexafluoride and Sulfur Tetrafluoride", J. Phys. Chem., Vol. 75, No. 23, pp. 3517–3523, 1971.

[80] R. W. Odom, D. L. Smith and J. H. Futrell, "A Study of Electron Attachment to SF_6 and Auto-Detachment and Stabilization of SF_6^-", J. Phys. B: Atom. Molec. Phys., Vol. 8, No. 8, pp. 1349–1366, 1975.

[81] L. G. Christophorou, "Electron Attachment and Detachment Processes in Electronegative Gases", Contrib. Plasma Phys., Vol. 27, No. 4, pp. 237–281, 1987.

[82] J. E. Delmore and A. D. Appelhans, "Measured Variation in the Autoneutralization Lifetime of SF_6^- by Direct Measurement of Neutral Density", J. Chem. Phys., Vol. 84, No. 11, pp. 6238–6246, 1986.

[83] M. S. Foster and J. Beauchamp, "Electron Attachment to Sulfur Hexafluoride: Formation of Stable SF_6^- at Low Pressure", Chem. Phys. Lett., Vol. 31, No. 3, pp. 482–486, 1975.

[84] Yicheng Wang, R. L. Champion, L. D. Doverspike, J. K. Olthoff and R. J. Van Brunt, "Collisional Electron Detachment and Decomposition Cross Sections for SF_6^-, SF_5^-, and F^- on SF_6 and Rare Gas Targets", J. Chem. Phys., Vol. 91, No. 4, pp. 2254–2260, 1989.

[85] M. S. Huq, L. D. Doverspike, R. L. Champion and V. A. Esaulov, "Total Electron Detachment Cross Sections for Collisions of H^- with He and F^- with Atomic and Molecular Targets", J. Phys. B: Atom. Mol. Phys., Vol. 15, pp. 951–959, 1982.

[86] J. K. Olthoff, R. J. Van Brunt, Yicheng Wang, R. L. Champion and L. D. Doverspike, "Collisional Electron Detachment and Decomposition Rates of SF_6^-, SF_5^-, and F^- in SF_6: Implications for Ion Transport and Electrical Discharges", J. Chem. Phys., Vol. 91, No. 4, pp. 2261–2268, 1989.

[87] B. C. O'Neill and J. D. Craggs, "Collisional Detachment of Electrons in Sulfurhexafluoride", J. Phys. B: Atom. Molec. Phys., Vol. 6, pp. 2634–2640, 1973.

[88] K. B. McAfee and D. Edelson, "Identification and Mobility of Ions in a Townsend Discharge by Time-resolved Mass Spectrometry", Proc. Phys. Soc. (London), Vol. 81, pp. 383–384, 1963.

[89] J. de Urquijo-Carmona, I. Alvarez, and C. Cisneros, "Time-Resolved Study of Charge Transfer in SF_6", J. Phys. D: Appl. Phys., Vol. 19, pp. L207–L210, 1986.

[90] Y. Nakamura and T. Kizu, "Reaction Coefficients of Negative Ions in SF_6", Proc. 5th Int. Swarm Seminar, Birmingham, UK, pp. 126–129 (1987).

[91] R. Morrow, "A Survey of the Electron and Ion Transport Properties of SF_6", IEEE Trans. Plasma Sci., Vol. 14, No. 3, pp. 234–239, 1986.

[92] K. P. Brand and J. Jungblut, "The Interaction Potentials of SF_6^- Ions in SF_6 Parent Gas Determined from Mobility Data", J. Chem. Phys., Vol. 78, No. 4, pp. 1999–2007, 1983.

[93] Y. Nakamura, "Transport Coefficients of Electrons and Negative Ions in SF_6", J. Phys. D: Appl. Phys., Vol. 21, pp. 67–72, 1988.

[94] D. Hansen, H. Jungblut and W. F. Schmidt, "Electron Detachment from Negative Ions in Sulfurhexafluoride", J. Phys. D: Appl. Phys., Vol. 16, pp. 1623–1634, 1983.

[95] N. Wiegart, "A Model for the Production of Initial Electrons by Detachment of SF_6^--Ions", IEEE Trans. Elec. Insul., Vol. 20, pp. 587–594, 1985.

[96] W. F. Schmidt and R. J. Van Brunt, "Comments on the Effect of Electron Detachment in Initiating Breakdown in Gaseous Dielectrics", in *Gaseous Dielectrics III*, (Proc. 3rd Int. Symp. on Gaseous Dielectrics) ed. L. G. Christophorou, Pergamon Press, New York, pp. 561–563, 1982.

[97] G. Riquel, B. Hutzler, G. Berger, B. Senouci and O. Belabed, "The Influence of Water Vapor on the Dielectric Strength of Sulfur Hexafluoride", Proc. 5th Int. Symp. on High Voltage Engineering, Braunschweig, West Germany, 1987.

[98] G. Berger and B. Senouci, "The Role of Impurities on the Deviation from Paschen's Law of SF_6", J. Phys. D: Appl. Phys., Vol. 19, pp. 2337–2342, 1986.

[99] B. Senouci, G. Berger, E. Marode, O. Belabed, I. Gallimberti and A. Osgualdo, "Similarity Law and Discharge Mechanisms in Pure, Natural and Moist SF_6 for Positive Polarity", Conf. Record 1988 IEEE Int. Symp. on Elec. Insul., IEEE, NY, pp 128–130, 1988.

[100] I. Sauers, M. C. Siddagangappa and G. Harman, "Influence of Water Vapor and Decomposition Products on the Positive-and Negative-Ion Spectra of SF_6 Corona", Proc. 6th Int. Symp. on High Voltage Engineering, New Orleans, LA, 1989.

[101] I. Sauers, "Sensitive Detection of Byproducts formed in Electrically Discharged SF_6", IEEE Trans. Elec. Insul., Vol. 21, pp. 105–110, 1986.

[102] L. M. Babcock and G. E. Streit, "Negative Ion-Molecule Reactions of SF_4", J. Chem. Phys., Vol. 75, No. 8, pp. 3864–3870, 1981.

[103] J. C. Haartz and D. H. McDaniel, "Fluoride Ion Affinity of Some Lewis Acids", J. Am. Chem. Soc., Vol. 95, pp. 8562–8565, 1973.

[104] J. W. Larson and T. B. McMahon, "Fluoride and Chloride Affinities of Main Group Oxides, Fluorides, Oxofluorides, and Alkyls. Quantitative Scales of Lewis Acidities from Ion Cyclotron Resonance Halide-Exchange Equilibria", J. Am. Chem. Soc., Vol. 107, pp. 766–773, 1985.

[105] I. Sauers, "Negative Ions in SF_6 Corona Discharges", Proc. 40th Annual Gaseous Electronics Conf., Bull. Am. Phys. Soc., Vol. 33, No. 2, pp. 135, 1988.

[106] G. Berger, *Retard a la Formation de la Decharge Couronne Positive dans l'Air*, Thesis, Université de Paris-Sud, Centre d'Orsay, 1980.

[107] L. W. Sieck, "Thermochemistry of Solvation of SF_6^- by Simple Polar Organic Molecules in the Vapor Phase", J. Phys. Chem., Vol. 90, pp. 6684–6687, 1986.

[108] P. L. Patterson, "Mobilities of Negative Ions in SF_6", J. Chem. Phys., Vol. 33, No. 2, pp. 696–704, 1970.

[109] S. Chowdhury and P. Kebarle, "Role of Binding Energies in $A^- \bullet B^-$ Complexes in the Kinetics of Gas Phase Electron Transfer Reactions: $A^- + B = A + B^-$ Involving Perfluoro Compounds: SF_6, $C_6F_{11}CF_3$, C_6F_6", J. Chem. Phys., Vol. 85, No. 9, pp. 4989–4994, 1986.

[110] K. Mitsuke, T. Kondow and K. Kuchitsu, "Formation of Negative Cluster Ions in Collisions of SF_6 Clusters with Krypton Rydberg Atoms", J. Phys. Chem., Vol. 90, pp. 1552–1556, 1986.

[111] R. J. Van Brunt and M. Misakian, "Mechanisms for Inception of DC and 60-Hz AC Corona in SF_6", IEEE Trans. Elec. Insul., Vol. 17, pp. 106–120, 1982.

[112] I. Sauers, J. L. Adcock, L. G. Christophorou and H. W. Ellis, "Gas-Phase Hydrolysis of Sulfur Tetrafluoride: A Comparison of the Gaseous and Liquid Phase Rate Constants", J. Chem. Phys. Vol. 83, No. 5, pp. 2618–2619, 1985.

[113] D. R. Johnson and F. X. Powell, "Microwave Spectrum and Structure of Sulfur Difluoride", Science, Vol. 164, pp. 950–951, 1969.

[114] R. D. Johnson and J. W. Hudgens, "Electronic Spectra of SF_2 Radicals Between 295 and 495 nm Observed with Resonance Enhanced Multiphoton Ionization Spectroscopy", J. Phys. Chem. (in press, 1990).

[115] F. Seel, E. Heinrich, W. Gombler and R. Budenz, "Sulfur Difluoride", Chimia, Vol. 23, pp. 73–74, 1969.

[116] R. J. Van Brunt and I. Sauers, "Gas-Phase Hydrolysis of SOF_2 and SOF_4", J. Chem. Phys., Vol. 85, No. 8, pp. 4377–4380, 1986.

[117] H. Latour-Slowikowska, J. Lampe and J. Slowikowski, "On Reactions Occurring in the Gaseous Phase in Decomposed SF_6", in *Gaseous Dielectrics V*, (Proc. 4th Int. Symp. on Gaseous Dielectrics) ed. L. G. Christophorou and M. O. Pace, Pergamon Press, New York, pp. 286–291, 1984.

[118] K. D. Asmus, W. Grunbein and J. H. Fendler, "Conductometric Radiolysis of Sulfurhexafluoride in Aqueous Solutions. Rate of Hydrolysis for Sulfur Tetrafluoride", J. Am. Chem. Soc., Vol. 92, No. 9, pp. 2625–2628, 1970.

[119] J. K. Olthoff, R. J. Van Brunt, J. T. Herron, I. Sauers and G. Harman, "Catalytic Decomposition of S_2F_{10} and its Implications on Sampling and Detection from SF_6-Insulated Equipment", Conf. Rec. 1990 IEEE Int. Symp. on Elec. Insul., IEEE, New York (in press, 1990).

Manuscript was received on 18 Oct 1989, in revised form 18 Dec 1989.